

Collective stochastic resonance behaviors of two coupled harmonic oscillators driven by dichotomous fluctuating frequency

Lei Jiang(姜磊), Li Lai(赖莉), Tao Yu(蔚涛), Maokang Luo(罗懋康)

Citation: Chin. Phys. B, 2021, 30 (**6**): 060502. DOI: 10.1088/1674-1056/abd9b0
Journal homepage: http://cpb.iphy.ac.cn; http://iopscience.iop.org/cpb

What follows is a list of articles you may be interested in

Synchronization mechanism of clapping rhythms in mutual interacting individuals

Shi-Lan Su(苏世兰), Jing-Hua Xiao(肖井华), Wei-Qing Liu(刘维清), and Ye Wu(吴晔)
Chin. Phys. B, 2021, 30 (**1**): 010505. DOI: 10.1088/1674-1056/abb30a

Relaxation dynamics of Kuramoto model with heterogeneous coupling

Tianwen Pan(潘天文), Xia Huang(黄霞), Can Xu(徐灿), Huaping Lü(吕华平)
Chin. Phys. B, 2019, 28 (**12**): 120503. DOI: 10.1088/1674-1056/ab55d0

Explosive synchronization of multi-layer frequency-weighted coupled complex systems

Yan-Liang Jin(金彦亮), Lin Yao(姚林), Wei-Si Guo(郭维思), Rui Wang(王瑞), Xue Wang(王雪), Xue-Tao Luo(罗雪涛)
Chin. Phys. B, 2019, 28 (**7**): 070502. DOI: 10.1088/1674-1056/28/7/070502

Energy feedback and synchronous dynamics of Hindmarsh-Rose neuron model with memristor

K Usha, P A Subha
Chin. Phys. B, 2019, 28 (**2**): 020502. DOI: 10.1088/1674-1056/28/2/020502

Double compound combination synchronization among eight *n*-dimensional chaotic systems

Gamal M Mahmoud, Tarek M Abed-Elhameed, Ahmed A Farghaly
Chin. Phys. B, 2018, 27 (**8**): 080502. DOI: 10.1088/1674-1056/27/8/080502

Collective stochastic resonance behaviors of two coupled harmonic oscillators driven by dichotomous fluctuating frequency*

Lei Jiang(姜磊)[1], Li Lai(赖莉)[1], Tao Yu(蔚涛)[1,†], Maokang Luo(罗懋康)[1,2]

[1] College of Mathematics, Sichuan University, Chengdu 610064, China
[2] College of Aeronautics and Astronautics, Sichuan University, Chengdu 610064, China

(Received 10 November 2020; revised manuscript received 3 January 2021; accepted manuscript online 8 January 2021)

The collective behaviors of two coupled harmonic oscillators with dichotomous fluctuating frequency are investigated, including stability, synchronization, and stochastic resonance (SR). First, the synchronization condition of the system is obtained. When this condition is satisfied, the mean-field behavior is consistent with any single particle behavior in the system. On this basis, the stability condition and the exact steady-state solution of the system are derived. Comparative analysis shows that, the stability condition is stronger than the synchronization condition, that is to say, when the stability condition is satisfied, the system is both synchronous and stable. Simulation analysis indicates that increasing the coupling strength will reduce the synchronization time. In weak coupling region, there is an optimal coupling strength that maximizes the output amplitude gain (OAG), thus the coupling-induced SR behavior occurs. In strong coupling region, the two particles are bounded as a whole, so that the coupling effect gradually disappears.

Keywords: coupled harmonic oscillators, dichotomous fluctuating frequency, synchronization, stability, stochastic resonance

PACS: 05.40.–a, 05.45.–a, 05.45.Xt, 05.90.+m **DOI:** 10.1088/1674-1056/abd9b0

1. Introduction

Stochastic resonance (SR) is one of several interesting phenomena, wherein the influence of noise is not restricted to destructive effects, but can have unanticipated ordered outcomes.[1–3] Counterintuitively, the output of such a noisy nonlinear dynamic system, driven by a weak periodic signal, can actually be amplified by a proper dose of noise. Three main ingredients (*i.e.*, nonlinearity, a weak periodic force, and a noise source) are required for the happening of SR. Early research of SR was confined to nonlinear systems driven by additive noise.[4–13] However, many recent investigations show that SR can also occur in linear systems with multiplicative colored noise.[14–24]

As a classical model, harmonic oscillators[25] are widely used to describe various natural phenomena. Thus, the research on harmonic oscillators have draw more and more attention. Especially, the SR of linear harmonic oscillators affected by complex environmental fluctuations has been widely investigated.[26–31] For example, Sauga[26] studied the resonant behavior of a fractional oscillator with fluctuating mass. Lang[27] investigated the SR of a linear system with random damping. Mankin[28] explored the SR of a harmonic oscillator with fluctuating frequency.

The above researches on SR mainly focused on uncoupled systems. However, in most stochastic dynamic systems, the particles are coupled in a complex network,[32] which means they may interact with each other. As the study of coupled system has continued to grow in importance and popularity, the SR investigation of coupled systems has become a hot research topic.[9–13,33] It was shown that the coupling can lead to the enrichment of the resonance behavior.[9,12,33] Pikovsky[12] demonstrated the existence of system size resonance in coupled noisy systems. The diversity-induced resonance in globally coupled bistable systems was researched in Ref. [9]. Nicolis[33] showed that nonlinear spatially coupled subsystems can induce coupling-enhanced SR.

In most previous studies, the impact of environmental fluctuations on each coupled particle is assumed to be identical,[17,19,31] which means the same noise will be added to each coupled oscillator. In realistic situations, although the coupled particles are in the same environment, the fluctuation noises acting on them are only independently and identically distributed, not exactly the same. Therefore, for coupled particles with independently and identically distributed noises, studying their collective SR behavior is an interesting problem.

As one of the most important noises, dichotomous noise has drawn great attention in theory and application. The widely application of dichotomous noise is due to its two properties. First, it is bounded, which makes it easy to be realized in physical and biological systems.[34–36] Second, dichotomous noise can be made by well-defined procedures to two limiting forms: Gaussian white noise and white shot noise, which is of great theoretical interest.[37]

In this paper, we study two coupled harmonic oscilla-

*Project supported by the National Natural Science Foundation of China for the Youth (Grant Nos. 11501385 and 11801385).
†Corresponding author. E-mail: scuyutao@163.com
© 2021 Chinese Physical Society and IOP Publishing Ltd

tors with different random frequency fluctuations, which are modeled as dichotomous noises. The two-coupled oscillators system can be regarded as a basic case of complex coupled systems, such as globally[13] and nearest-neighbor[33] coupled systems. Related studies[38–40] show that this kind of system can exhibit rich nonlinear dynamic behaviors and provide theoretical guidance for related investigations on complex systems. Through the Shapiro–Loginov formula[41] and the Routh–Hurwitz stability criterion,[42] we obtain the synchronization condition of the system. Based on this, the stability condition and the exact steady-state solution are derived. Finally, the collective behaviors of the coupled system are analyzed through theoretical and numerical methods, including stability, synchronization, and SR.

The remainder of our paper is organized as follows. In Section 2, we introduce the model of two coupled harmonic oscillators with fluctuating frequency. In Section 3, we derive the corresponding analytical results. The numerical simulation method is given in Section 4. In Section 5, the collective behaviors of the system are studied. The main conclusions of this paper are given in Section 6.

2. System model

2.1. The overdamped Langevin equation

In order to better explain the physical meaning of model (2), we first make a brief review of the related research on the overdamped Langevin equation

$$\frac{\mathrm{d}x(t)}{\mathrm{d}t} = -(\omega + \xi(t))x(t) + F(t), \tag{1}$$

where $x(t)$ represents the position of the particle at time t. ω is the eigenfrequency, and its fluctuation is modeled as noise term $\xi(t)$. $F(t)$ is the external force, usually taken as the sine $(A_0 \sin(\Omega t))$ or cosine $(A_0 \cos(\Omega t))$ periodic force.

Because of the wide application of Eq. (1) in many fields such as fluctuating barrier crossing,[43] enzimatic kinetics,[44] and nuclear magnetic resonance,[45] it has been extensively investigated. Berdichevsky *et al.*[46] firstly gave the analytical solution of Eq. (1) when $\xi(t)$ is modeled as symmetric dichotomous noise, and analyzed the SR phenomenon of this model. After that, the authors in Refs. [16,47] extend the above results to the case of asymmetric dichotomous noise, and give some new applications of Eq. (1) in first-order linear circuit.

2.2. The overdamped coupled system

Most dynamic models in biology, physics, or engineering are complex systems composed of multiple interacting particles. And the coupling effect makes the system exhibit many new dynamic behaviors. However, due to nonlinearity and complexity, most complex coupled systems can only be analyzed by numerical simulation. As the simplest coupled case, the two coupled oscillators system can be regarded as a basic unit of complex coupled systems, such as globally and nearest-neighbor coupled systems, and in many cases it can be solved theoretically. Thus, the study of such systems can provide theoretical guidance for the research of complex systems. Based on this, in this section we consider a coupled harmonic oscillators system consisting of two particles. The system is driven by a periodic cosine force. Random frequency fluctuation is modeled as the symmetric dichotomous noise. The system can be described as follows:

$$\frac{\mathrm{d}x_1}{\mathrm{d}t} + (\omega + \xi_1(t))x_1 = \varepsilon(x_2 - x_1) + A_0 \cos(\Omega t), \tag{2a}$$

$$\frac{\mathrm{d}x_2}{\mathrm{d}t} + (\omega + \xi_2(t))x_2 = \varepsilon(x_1 - x_2) + A_0 \cos(\Omega t), \tag{2b}$$

where x_i $(i = 1,2)$ represents the position of the i-th particle. $\varepsilon \geqslant 0$ is the coupling coefficient. Random frequency fluctuation is modeled as the symmetric dichotomous noise $\xi_i(t)$ $(i = 1,2)$. Each $\xi_i(t)$ $(i = 1,2)$ is a two-state Markov process with random values between $\pm\sigma$, which satisfies

$$\begin{aligned} &\langle \xi_i(t) \rangle = 0, \\ &\langle \xi_i(t)\xi_i(s) \rangle = \sigma^2 \mathrm{e}^{-\lambda|t-s|}, \end{aligned} \tag{3}$$

where $\langle \cdot \rangle$ represents statistical average, σ is the noise amplitude and λ represents the transition rate. Here, we assume that $\xi_1(t)$ and $\xi_2(t)$ are independent of each other.

Due to the random fluctuation of noise $\xi_i(t)$, the potential field of system (2) randomly switches between

$$V_{\pm}(x_i) = (\omega \pm \sigma)\frac{x_i^2}{2}. \tag{4}$$

This kind of fluctuating potential energy can be found in many systems. For example, in an ATP-ADP cycle system, ATP stores energy in its bond. By hydrolyze this bond, some electrons in the bond can enter into a lower energy state. That will result with some energy and ADP being put into the biological organism. Conversely, ADP can also generate ADT by using some energy.[48–50] Thus, system (2) can be viewed as the basic case of coupled protein molecular motor in the ATP-ADP potential field driven by a periodic cosine force.[31] Because in biological organism, ATP-ADP conversions do not all happen at the same time. Therefore, unlike Ref. [31], we assume that the fluctuations $\xi_i(t)$ $(i = 1,2)$ of the potential field are independent of each other. The authors in Ref. [19] proposes some potential applications of this type of coupled system.[51–54]

3. Theoretical analysis and results

3.1. Synchronization

In the following theoretical derivation part, the Shapiro–Loginov formulas will paly an important role, so we list them

here

$$\left\langle \xi_j \frac{\mathrm{d}x_i}{\mathrm{d}t} \right\rangle = \frac{\mathrm{d}\langle \xi_j x_i \rangle}{\mathrm{d}t} + \lambda \langle \xi_j x_i \rangle,$$
$$\left\langle \xi_1 \xi_2 \frac{\mathrm{d}x_i}{\mathrm{d}t} \right\rangle = \frac{\mathrm{d}\langle \xi_1 \xi_2 x_i \rangle}{\mathrm{d}t} + 2\lambda \langle \xi_1 \xi_2 x_i \rangle. \tag{5}$$

In order to study the collective behaviors of the coupled system, it is necessary to analyze the synchronization between x_1 and x_2, for which the solution of $\langle x_1 - x_2 \rangle$ is requisite. By subtracting Eq. (2b) from Eq. (2a), we obtain

$$\left(\frac{\mathrm{d}}{\mathrm{d}t} + \omega + 2\varepsilon\right)(x_1 - x_2) + (\xi_1 x_1 - \xi_2 x_2) = 0. \tag{6}$$

Taking average of Eq. (6), we have

$$\left(\frac{\mathrm{d}}{\mathrm{d}t} + \omega + 2\varepsilon\right)\langle x_1 - x_2 \rangle + \langle \xi_1 x_1 - \xi_2 x_2 \rangle = 0. \tag{7}$$

Equation (7) shows a new variable $\langle \xi_1 x_1 - \xi_2 x_2 \rangle$ waiting to be solved. Multiplying Eq. (6) by $\xi_1 + \xi_2$, we obtain

$$\left[\left(\frac{\mathrm{d}}{\mathrm{d}t} + \omega + 2\varepsilon\right)(x_1 - x_2)\right] \times (\xi_1 + \xi_2) + (\xi_1 x_1 - \xi_2 x_2)(\xi_1 + \xi_2) = 0. \tag{8}$$

Taking average of Eq. (8) and using Eq. (5), we have

$$\left(\frac{\mathrm{d}}{\mathrm{d}t} + \lambda + \omega + 2\varepsilon\right)(\langle \xi_1 x_1 - \xi_2 x_2 \rangle + \langle \xi_2 x_1 - \xi_1 x_2 \rangle) + \sigma^2 \langle x_1 - x_2 \rangle + \langle \xi_1 \xi_2 (x_1 - x_2) \rangle = 0. \tag{9}$$

There are two new variables $\langle \xi_2 x_1 - \xi_1 x_2 \rangle$, $\langle \xi_1 \xi_2 (x_1 - x_2) \rangle$ appearing in Eq. (9). In order to solve these two variables, multiplying Eq. (6) by $\xi_1 \xi_2$ and taking average yield

$$\left[\left(\frac{\mathrm{d}}{\mathrm{d}t} + 2\lambda\right) + \omega + 2\varepsilon\right]\langle \xi_1 \xi_2 (x_1 - x_2) \rangle + \sigma^2 \langle \xi_2 x_1 - \xi_1 x_2 \rangle = 0. \tag{10}$$

Multiplying Eq. (2a) by ξ_1 and Eq. (2b) by ξ_2, then subtracting the two results and averaging yield

$$\left[\left(\frac{\mathrm{d}}{\mathrm{d}t} + \lambda\right) + \omega + \varepsilon\right]\langle \xi_1 x_1 - \xi_2 x_2 \rangle + \sigma^2 \langle x_1 - x_2 \rangle + \varepsilon \langle \xi_2 x_1 - \xi_1 x_2 \rangle = 0. \tag{11}$$

Now, we have a set of ordinary differential equations [Eqs. (7), (9), (10), (11)], namely, synchronous equation set (SES), with four variables

$$z_1 = \langle x_1 - x_2 \rangle, \quad z_2 = \langle \xi_1 x_1 - \xi_2 x_2 \rangle,$$
$$z_3 = \langle \xi_2 x_1 - \xi_1 x_2 \rangle, \quad z_4 = \langle \xi_1 \xi_2 (x_1 - x_2) \rangle. \tag{12}$$

Based on the Routh–Hurwitz stability criterion, we derive the stability condition of the SES as follows:

$$\sigma < \sigma^* = \sqrt{(\lambda + 2\varepsilon + \omega)(\lambda + \varepsilon + \omega) - \sqrt{(\lambda + 2\varepsilon + \omega)(2\varepsilon^3 + (\lambda + \omega)\varepsilon^2 + \lambda^2(\lambda + \omega))}}. \tag{13}$$

The detailed derivation of the inequality (13) is given in Appendix A.

Next, we will solve the SES when the condition (13) is satisfied, that is, find the steady-state solution of the SES. In this situation, the influence of the initial value will vanish as $t \to \infty$. So, without loss of generality, the initial value is set to zero. Taking Laplace transform to be the SES, we have

$$\begin{cases} b_{11} Z_1 + b_{12} Z_2 = 0, \\ b_{21} Z_1 + b_{22} Z_2 + b_{23} Z_3 + b_{24} Z_4 = 0, \\ b_{33} Z_3 + b_{34} Z_4 = 0, \\ b_{41} Z_1 + b_{42} Z_2 + b_{43} Z_3 = 0, \end{cases} \tag{14}$$

where $Z_i(s) = L(z_i) = \int_0^\infty z_i(t)\, \mathrm{e}^{-st}\, \mathrm{d}t$, $i = 1, 2, 3, 4$.

$$b_{11} = s + \omega + 2\varepsilon, \quad b_{12} = 1,$$
$$b_{21} = \sigma^2, \quad b_{22} = s + \lambda + \omega + 2\varepsilon, \quad b_{23} = b_{22},$$
$$b_{24} = 1, \quad b_{33} = \sigma^2, \quad b_{34} = s + 2\lambda + \omega + 2\varepsilon,$$
$$b_{41} = \sigma^2, \quad b_{42} = s + \lambda + \omega + \varepsilon, \quad b_{43} = \varepsilon. \tag{15}$$

Solving Eq. (14), we have

$$Z_1(s) = Z_2(s) = Z_3(s) = Z_4(s) = 0. \tag{16}$$

Applying the inverse Laplace transform to Eq. (16), we obtain

$$\langle x_1 \rangle = \langle x_2 \rangle, \quad \langle \xi_1 x_1 \rangle = \langle \xi_2 x_2 \rangle,$$
$$\langle \xi_2 x_1 \rangle = \langle \xi_1 x_2 \rangle, \quad \langle \xi_1 \xi_2 x_1 \rangle = \langle \xi_1 \xi_2 x_2 \rangle. \tag{17}$$

It can be seen from Eq. (17) that the average motions of the two particles are synchronized. So, inequality (13) is named the synchronization condition, that is to say, when inequality (13) is satisfied, the two particles are synchronized. The synchronization between particles makes the mean-field behavior consistent with any single particle behavior in the coupled system. So, in order to analyze the collective behaviors of the system, we only need to consider the first particle's behaviors below.

3.2. The stability condition and output amplitude gain

In order to obtain the analytical expression of $\langle x_1 \rangle$, averaging Eq. (2a), then using Eq. (17), we have

$$\left(\frac{\mathrm{d}}{\mathrm{d}t} + \omega\right)\langle x_1 \rangle + \langle \xi_1 x_1 \rangle = A_0 \cos(\Omega t). \tag{18}$$

A new variable $\langle \xi_1 x_1 \rangle$ appears in Eq. (18). In order to solve this variable, multiplying Eq. (2a) by ξ_1 and averaging, we

have

$$\left(\frac{\mathrm{d}}{\mathrm{d}t}+\lambda+\omega+\varepsilon\right)\langle\xi_1 x_1\rangle+\sigma^2\langle x_1\rangle-\varepsilon\langle\xi_2 x_1\rangle=0. \quad (19)$$

Similarly, in order to solve $\langle\xi_2 x_1\rangle$, multiplying Eq. (2a) by ξ_2 and averaging, we obtain

$$\left(\frac{\mathrm{d}}{\mathrm{d}t}+\lambda+\omega+\varepsilon\right)\langle\xi_2 x_1\rangle-\varepsilon\langle\xi_1 x_1\rangle+\langle\xi_1\xi_2 x_1\rangle=0. \quad (20)$$

To solve $\langle\xi_1\xi_2 x_1\rangle$, multiplying Eq. (2a) by $\xi_1\xi_2$ and averaging, we get

$$\left(\frac{\mathrm{d}}{\mathrm{d}t}+2\lambda+\omega\right)\langle\xi_1\xi_2 x_1\rangle+\sigma^2\langle\xi_2 x_1\rangle=0. \quad (21)$$

Now, we get a closed set of equations [Eqs. (18)–(21)], namely, OAG equation set (OAGES), for four variables:

$$\begin{aligned} y_1&=\langle x_1\rangle,\\ y_2&=\langle\xi_1 x_1\rangle,\\ y_3&=\langle\xi_2 x_1\rangle,\\ y_4&=\langle\xi_1\xi_2 x_1\rangle. \end{aligned} \quad (22)$$

Based on the Routh–Hurwitz stability criterion, the stability condition for the OAGES can be written as follows:

$$\sigma<\sigma^{**}=\sqrt{(\lambda+\omega)(\lambda+\omega+\varepsilon)-\sqrt{(\lambda^3+(\omega+2\varepsilon)\lambda^2+\varepsilon^2\lambda+\varepsilon^2\omega)(\lambda+\omega)}}. \quad (23)$$

We call inequality (23) the stability condition. The concrete derivation is given in Appendix B.

Next, we will solve the OAGES with the stability condition (23) satisfied. Without loss of generality, the initial conditions are assumed to be zero. Using the Laplace transform technique, we obtain

$$\begin{cases} a_{11}Y_1+a_{12}Y_2=A_0\dfrac{s^2}{s^2+\Omega^2},\\ a_{21}Y_1+a_{22}Y_2+a_{23}Y_3=0,\\ a_{32}Y_2+a_{33}Y_3+a_{34}Y_4=0,\\ a_{43}Y_3+a_{44}Y_4=0, \end{cases} \quad (24)$$

where $Y_i(s)=L(y_i)=\int_0^\infty y_i(t)\,\mathrm{e}^{-st}\,\mathrm{d}t$, $i=1,2,3,4$.

$$\begin{aligned} &a_{11}=s+\omega, \quad a_{12}=1,\\ &a_{21}=\sigma^2, \quad a_{22}=s+\lambda+\omega+\varepsilon, \quad a_{23}=-\varepsilon,\\ &a_{32}=-\varepsilon, \quad a_{33}=s+\lambda+\omega+\varepsilon, \quad a_{34}=1,\\ &a_{43}=\sigma^2, \quad a_{44}=s+2\lambda+\omega. \end{aligned} \quad (25)$$

Solving Eqs. (24), we have

$$Y_1(s)=H_1(s)A_0\frac{s^2}{s^2+\Omega^2}, \quad (26)$$

where

$$\begin{aligned} H_1(s)&=\frac{g(s)}{f(s)},\\ g(s)&=a_{22}a_{33}a_{44}-a_{22}a_{34}a_{43}-a_{23}a_{32}a_{44},\\ f(s)&=a_{11}a_{22}a_{33}a_{44}-a_{11}a_{22}a_{34}a_{43}-a_{11}a_{23}a_{32}a_{44}\\ &\quad -a_{12}a_{21}a_{33}a_{44}+a_{12}a_{21}a_{34}a_{43}. \end{aligned} \quad (27)$$

Applying the inverse Laplace transform technique to Eq. (26), we obtain the steady state-solution of Eq. (2a) as follows:

$$\langle x_1\rangle=A_0\int_0^t h_1(t-\tau)\cos(\Omega\tau)\,\mathrm{d}\tau, \quad (28)$$

where $h_1(t)$ is the inverse Laplace transform of $H_1(s)$.

On the other hand, we can also solve $\langle x_1\rangle$ through the linear response theory. Since the input of Eq. (26) is a cosine signal, the system response should also be a cosine signal that differs from the input signal only in amplitude and phase angle. So we have

$$\langle x_1\rangle=A\cos(\Omega t+\phi), \quad (29)$$

where A and ϕ are the amplitude and the phase angle of $\langle x_1\rangle$, respectively. Taking Laplace transform to Eq. (29) and comparing to Eq. (26) with $s=j\Omega$, we have

$$A=A_0|H_1(j\Omega)|, \quad \phi=\arg(H_1(j\Omega)). \quad (30)$$

According to its definition, the output amplitude gain (OAG) can be written as follows:

$$G=\frac{A}{A_0}=|H_1(j\Omega)|. \quad (31)$$

From inequality (23) and Eq. (31), we can see that the coupling strength will affect the stability region and the OAG of the system. This is mainly caused by the different random fluctuations. When the noises are identical, the effect of coupling strength disappears.[31] Therefore, compared with some existing works, we think our results can reflect better the influence of the interaction between particles, *i.e.*, coupling strength, on the collective behavior of the system. This is also one of the main results of this article.

3.3. Stability analysis

As can be seen from the inequality (23), the stability of the system is mainly determined by the value of σ. When σ is smaller than a certain critical value σ^{**}, the system is stable. This is because the potential field of system (2) randomly switches between $V_\pm(x_i)$. Note that (i) for $0<\sigma<\omega$, both $V_+(x_i)$ and $V_-(x_i)$ are in steady states, and (ii) for $0<\omega<\sigma$, $V_+(x_i)$ is stable and $V_-(x_i)$ is unstable. Direct calculations indicate that the right side of the inequality (23) is greater than

ω. So the stability of the system is not obvious. According to the physical meaning of (i), when $\sigma < \omega$, affected by the potential field force, particles will have a tendency to slide to the bottom of the potential field. This tendency leads to the stability of system (2). Meanwhile, it can be seen from inequality (23) that σ^{**} increases with the increase of ω, and when $\omega = 0, \sigma^{**} = 0$. Through the above analysis, it can be obtained that among all the parameters, the stability range (inequality (23)) of the system (2) is mainly affected by ω.

Since $\lambda, \omega, \varepsilon$ are all positive numbers, direct calculation shows that the stability condition is stronger than the synchronization condition, that is, for any positive numbers $\lambda, \omega, \varepsilon$,

$$\sigma^{**} < \sigma^{*}. \tag{32}$$

The concrete derivation is given in Appendix C. Inequality (32) shows that if system (2) is stable then the two particles must be synchronized. Due to the inclusion relationship represented by inequality (32), below we mainly discuss the two particles' behaviors when the stability condition (23) is satisfied.

4. Numerical simulation method

The numerical simulation method used in this article is stochastic Taylor expansion. For sufficiently small time step Δt, the discrete time representation of the system (2) can be written as follows:

$$\begin{aligned} &x_i(t_n) = x_i(t_{n-1}) + f_i(t_{n-1})\Delta t - x_i(t_{n-1})\Delta X_i(t_{n-1}), \\ &i = 1, 2, \end{aligned} \tag{33}$$

where

$$\begin{aligned} f_i(t_{n-1}) &= -\omega x_i(t_{n-1}) + \varepsilon \sum_{j=1}^{2} (x_j(t_{n-1}) - x_i(t_{n-1})) \\ &\quad + A_0 \cos(\Omega t_{n-1}), \\ \Delta X_i(t_{n-1}) &= \int_{t_{n-1}}^{t_n} \xi_i(u)\mathrm{d}u, \end{aligned} \tag{34}$$

and ΔX_i is simulated by the method described in Ref. [55].

In this study, we focus on the average displacement $\langle x_i(t)\rangle$, which can be approximated by Monte Carlo method as follows:

$$\langle x_i(t)\rangle = \frac{1}{K}\sum_{k=1}^{K} x_i^k(t), \tag{35}$$

$$\tag{36}$$

where $x_i^k(t)$ denotes displacement of the i-th particle in the k-th realization and K is the number of the realizations.

To verify the effectiveness of this algorithm, we need to compare the simulation result with theoretical value. According to Eq. (29), $\langle x_i(t)\rangle$ is a cosine signal with the same frequency as the input signal $A_0 \cos \Omega t$. The theoretical value of G is given in Eq. (31). Meanwhile, we can obtain the simulation output amplitude A by performing Fourier transform on the numerical result obtained by Eq. (35), which corresponds to the first panel of Fig. 1. The first panel of Fig. 1 is a concrete realization of $\langle x_i(t)\rangle$. As shown in the bottom panel of Fig. 1, the numerical result $\hat{G} = A/A_0 = 0.4388$ is consistent with the theoretical result $G = 0.43906$. The relative error is only -5.9217×10^{-4}, which is mainly affected by the number (K) of Monte Carlo simulations and the time step Δt.

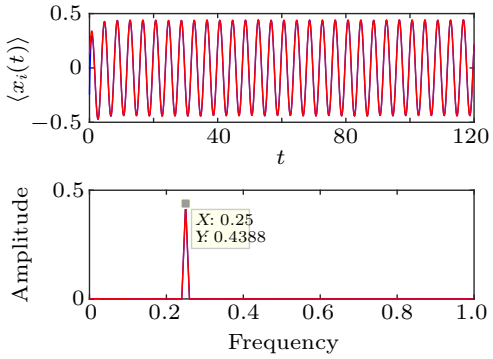


Fig. 1. The average realization and the corresponding frequency domain representation with $\varepsilon = 1, A_0 = 1, \sigma = 2, \omega = 2, \lambda = 0.9, \Omega = \pi/2, \Delta t = 10^{-3}$, $N = 10^4$. Different colors represent the two different particles.

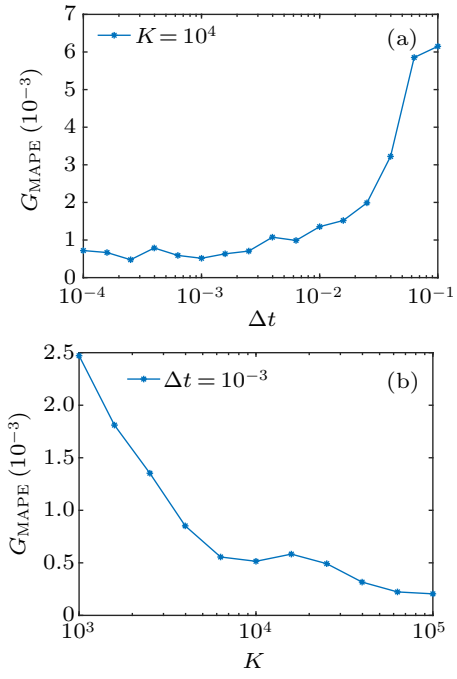


Fig. 2. The mean absolute percentage error with the system parameters being the same as Fig. 1, (a) as a function of Δt with $K = 10^4$ and (b) as a function of K with $\Delta t = 10^{-3}$.

To better reflect the effect of simulation parameters on error, the following mean absolute percentage error is considered:

$$G_{\mathrm{MAPE}} = \frac{1}{N}\sum_{j=1}^{N}\left|\frac{\hat{G}_j - G}{G}\right|. \tag{37}$$

Under the same system parameters and simulation parameters, the above simulation process is repeated N times, and then N simulation values $\hat{G}_j$, $(j = 1, 2, \ldots, N)$ are obtained. G is the

theoretical value given by Eq. (31). Below, we take $N = 10$ for simulation analysis.

Figure 2 shows the trend of G_{MAPE} with the time step Δt and the simulation number K. From Fig. 2(a), we can see that G_{MAPE} decreases with the decreasing of Δt. And the simulation results will not depend on Δt when $\Delta t \leq 10^{-2.6}$. From Fig. 2(b), we can see that G_{MAPE} decreases with the increasing of K. When $K = 10^4$, $G_{\mathrm{MAPE}} = 5.147 \times 10^{-4}$, which has meet the accuracy requirements. So, in all subsequent simulations, the time step Δt and the simulation number K are set to be 10^{-3} and 10^4, respectively.

5. Particle behavior analysis

5.1. The effect of stable region

In Section 3, the theoretical solution is derived on the premise that the stability condition (23) is satisfied. So we need to analyze the influence of the stability condition on the particle's motion behavior. To this end, figure 3 provides the stable region in the σ–ε plane. From Fig. 3, we can see that the σ–ε plane is divided into two regions. The black region is the stable region which means the stability condition (23) holds, while the white area represents the unstable region.

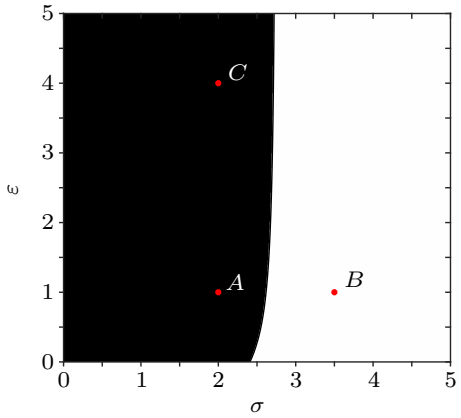


Fig. 3. The stable region in σ–ε plane with $\omega = 2$, $\lambda = 0.9$.

To intuitively show the effect of the stability condition on system (2), we choose one point $A = (2,1)$ in the stable region and one point $B = (3.5,1)$ in the unstable region. Figure 4 illustrates the average displacements of the two particles with different noise intensities σ. The initial positions of the two particles are random variables obeying normal distribution with mean 0 and standard deviation 0.5.

A stable system is a dynamic system with a bounded response to a bounded input.[42] From the simulations in Fig. 4(a), we observe that the average particle displacements are bound and significantly smaller than that in Fig. 4(b). In Fig. 4(b), the system response is unbounded, which means the system is unstable. This is consistent with the conclusion given in Fig. 3.

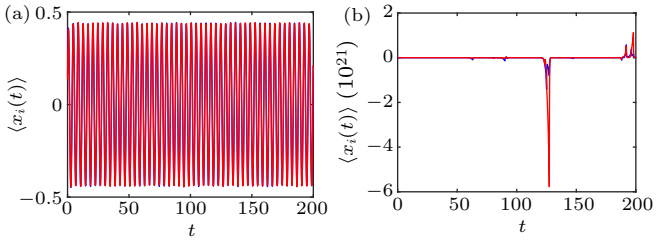


Fig. 4. Average displacements of the two particles with $\omega = 2$, $\lambda = 0.9$, $A_0 = 1$, $\varepsilon = 1$, $\Omega = \pi/2$ for (a) $\sigma = 2$ and (b) $\sigma = 3.5$.

5.2. Synchronization

From the inequality (32), it can be seen that when the particles meet the stability condition (23), the average motions of the two particles tend to be synchronized after a period of time. In order to analyze the effect of coupling on particle synchronization, we select two points ($A = (2,1)$, $C = (2,4)$) with different coupling strengths in the stable region of Fig. 3. The corresponding numerical results are given in Fig. 5.

Figure 5 shows the average displacements of the two particles and the corresponding variances. In the first panel of Figs. 5(a) and 5(b), the average displacement values of the two particles are depicted. It can be seen that, for different ε, the two particles will be synchronized after a period of time. And the particles in Fig. 5(a) enter the synchronization state faster than that in Fig. 5(b). This indicates that increasing the coupling strength will reduce the synchronization time. To further analyze the synchronization time, we define the variance $\Delta(t)$ of the average displacements as follows:

$$\Delta(t) = \frac{1}{2}\sum_{i=1}^{2}(\langle x_i(t)\rangle - \langle \bar{x}(t)\rangle)^2, \tag{38}$$

where

$$\langle \bar{x}(t)\rangle = \frac{1}{2K}\sum_{k=1}^{K}\sum_{i=1}^{2} x_i^k(t). \tag{39}$$

The second panel of Figs. 5(a) and 5(b) depicts $\Delta(t)$ as a function of t. We can intuitively see that $\Delta(t)$ falls faster in Fig. 5(b) than in Fig. 5(a). When $t = 2$, $\Delta = 1.1 \times 10^{-5}$ in Fig. 5(a), while $\Delta = 1.571 \times 10^{-7}$ in Fig. 5(b). To further clarify the difference, we use log-log plot to redraw the two figures in the third panel. In the two new figures, $\Delta(t)$ monotonically decreasing at the beginning, then it began to randomly fluctuate after falling below a certain value. This phenomenon can be explained as follows: The potential energy of the i-th particle is $(\omega + \xi_i)x_i^2/2$, and the potential field force it receives is $(\omega + \xi_i)x_i$. Since the noise ξ_i $(i = 1,2)$ are independent of each other and the number (K) of realizations is limited, the difference between the two random potential field forces cannot be completely eliminated, thereby hindering the further reduce of the Δ. In fact, we have verified through simulation that when $\xi_1 = \xi_2$, even if $K = 1$, the displacements of the two particles

can be completely synchronized ($\Delta < 10^{-30}$). In order to illustrate the synchronization time in quantity, we set a threshold $\Delta^* = 10^{-4}$. When $\Delta < \Delta^*$, we assume that the two particles are synchronized. We define

$$t_0 = \max\{t|\Delta(t) \geq \Delta^*\} \tag{40}$$

as the synchronization time. Then the synchronization times in Figs. 5(a) and 5(b) are 1.276 and 0.26, respectively.

To further illuminate the effect of coupling on particle synchronization, we depicts the variance Δ as a function of the time t and the coupling strength ε in Fig. 6(a) and depicts the corresponding synchronization time t_0 as the function of the coupling strength ε in Fig. 6(b). From this we can see that, although the particles will synchronize eventually, the coupling strength ε will affect the synchronization time t_0. The synchronization time decreases with the increasing of ε. But the rate of decline gets slower and slower.

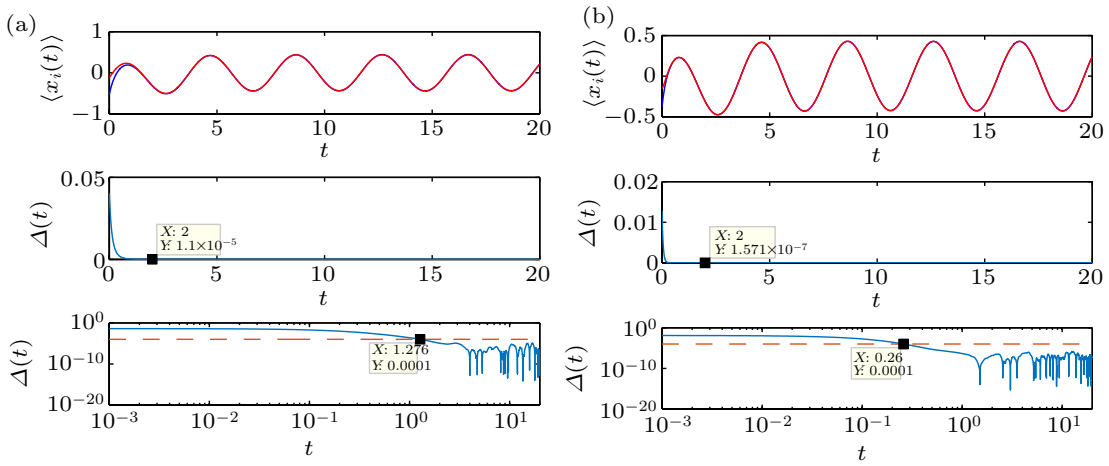


Fig. 5. The average displacements of two particles and the corresponding variances with $\omega = 2$, $\lambda = 0.9$, $\sigma = 2$, $A_0 = 1$, $\Omega = \pi/2$ for (a) $\varepsilon = 1$ and (b) $\varepsilon = 4$.

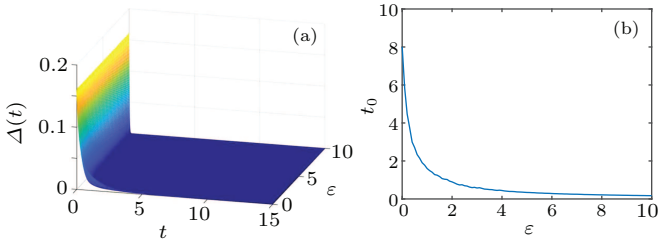


Fig. 6. Dependence of synchronization time on the coupling strength with $\omega = 2$, $\lambda = 0.9$, $A_0 = 1$, $\sigma = 2$, $\Omega = \pi/2$. (a) The variance Δ as a function of t and ε; (b) the synchronization time t_0 as a function of ε.

5.3. Stochastic resonance

SR is the result of the cooperation between the randomness of noise and the orderliness of driving forces under nonlinear action. In our model, the randomness is provided by noise, and the orderliness is yielded by three parts: cosine driving force, coupling force and potential field force generated by frequency ω, *i.e.*, ωx_i. Since the effect of cosine driving force has been extensively discussed in the previous literature, this article mainly analyzes the cooperation phenomenon of noise, coupling force. The mechanism of their cooperation to produce SR is as follows: The noises ξ_i, $(i = 1, 2)$ provide randomness to the system through the random fluctuation of the potential field. The system potential field switches randomly between $V_+(x_i)$ and $V_-(x_i)$. $V_+(x_i)$ makes the i-th particle have a tendency to slide to the bottom of the potential field, and $V_-(x_i)$ will slow down this trend and even make the i-th particle slide to infinity ($\sigma > \omega$). Therefore, frequency ω reduces the randomness caused by noise by weakening the amplification effect of $V_-(x_i)$. The coupling forces $\pm\varepsilon(x_1 - x_2)$ make the two particles attract each other and move synchronously to provide orderliness for the system. The greater the coupling strength ε, the stronger the orderliness. Under the nonlinear action mode of "multiplicativeness", orderliness and randomness compete with each other. When the two reach a certain optimal match, the SR occurs, which maximizes the output of the system. Next, we analyze the effect of coupling and noise on the resonance behavior of OAG obtained in Eq. (31).

Firstly, we analyze the influence of coupling strength ε on OAG under different noise amplitude σ. Figure 7(a) plots the curves of OAG as a function of ε when σ takes different values. It can be seen that when $\sigma = 0$, G takes a constant value, which means that the coupling has no effect on OAG. This is because, when $\sigma = 0$, the noise disappears, and system (2) becomes a deterministic system. The statistical synchronization ($\langle x_1\rangle = \langle x_2\rangle$) between two particles becomes traditional synchronization ($x_1 = x_2$). Therefore, the coupling forces $\varepsilon(x_1 - x_2)$ and $\varepsilon(x_2 - x_1)$ disappear, and the effect of the coupling disappears. In fact, when $\sigma = 0$, direct calculation can get $H_1(j\Omega) = 1/(\omega + j\Omega)$. So, $G = |H_1(j\Omega)|$ has no relationship with the coupling coefficient ε in this situation. When σ is greater than 0, the curves $G(\varepsilon)$ show a single-peak resonance. This indicates that there is an optimal cou-

pling strength which maximizes the OAG. As ε continues to increase, G will converge to a limit value. This is because, in strong coupling region, the two particles are bounded as a whole, so that the effect of coupling gradually disappears. As σ increases, the peak values first increase and then decrease. This indicates that the resonance intensity can be controlled by adjusting the noise amplitude, and there is an optimal noise amplitude to maximize the resonance intensity.

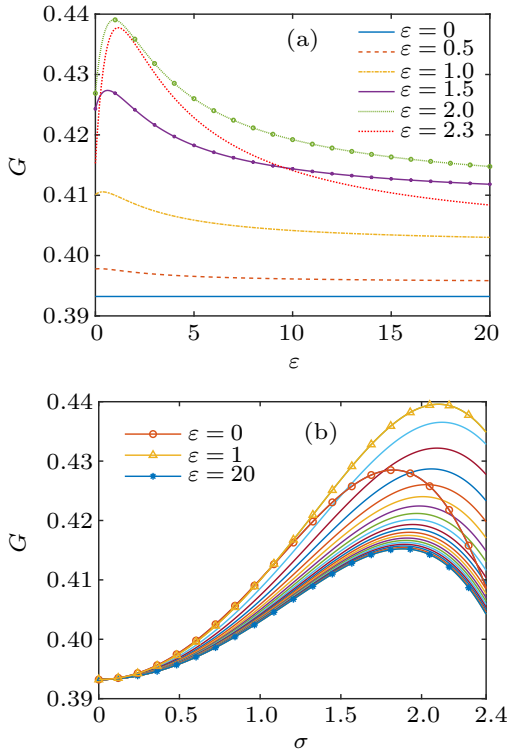


Fig. 7. The OAG *versus* noise amplitude σ and coupling strength ε with $\Omega = \pi/2$, $\omega = 2$, $\lambda = 0.9$, $A_0 = 1$. (a) Parameter-induced stochastic resonance (PSR) *versus* coupling strength ε; (b) SR *versus* noise amplitude σ, different colored curves represent different coupling strength ε from 0 to 20.

Secondly, we analyze the effect of the noise amplitude σ on OAG under different coupling strength ε. Figure 7(b) plots the curves of G as a function of σ when ε takes different values. It can be seen that single-peak resonance occurs. As ε increases, the peak values increase first and then decrease. This indicates that there is an optimal coupling strength which maximizes the resonance intensity. In addition, when ε increases, the curves gradually coincides, that is to say, when ε is large enough, continuing to increase ε will have no changes. This is consistent with the conclusion given in Fig. 7(a).

Finally, we have to point out that the reasons for SR in Figs. 7(a) and 7(b) are slightly different. In Fig. 7(a), two independent noises introduce different randomness to the trajectories of the two particles. This difference keeps the effect of coupling strength from disappearing over time. And from Eq. (31) we can also see that although the difference in the trajectory of the two particles can be eliminated by averaging, the ε has always had an impact on the particles trajectories. This indicates that the SR *versus* ε is mainly caused by the difference between the two noises. When the two noises are identical, the SR will disappear.[31] However, we can see from Fig. 7(b) that even if the coupling between the two particles disappears ($\varepsilon = 0$), which is equivalent to the two noises being identical, the system still exhibits SR. This shows that no matter whether the two noises are identical, the randomness introduced by the two noises will cause the system to produce SR *versus* σ.

Finally, some numerical simulations are given to verify the above theoretical results. Figure 8 is a comparison diagram of the theoretical results and the simulation results. It can be seen that the theoretical results are basically consistent with the simulations. Due to the greater noise amplitude will bring more randomness, the simulation error increases slightly with the growth of σ in Fig. 8(b). All the numerical simulations provide a good insight into the theoretical results.

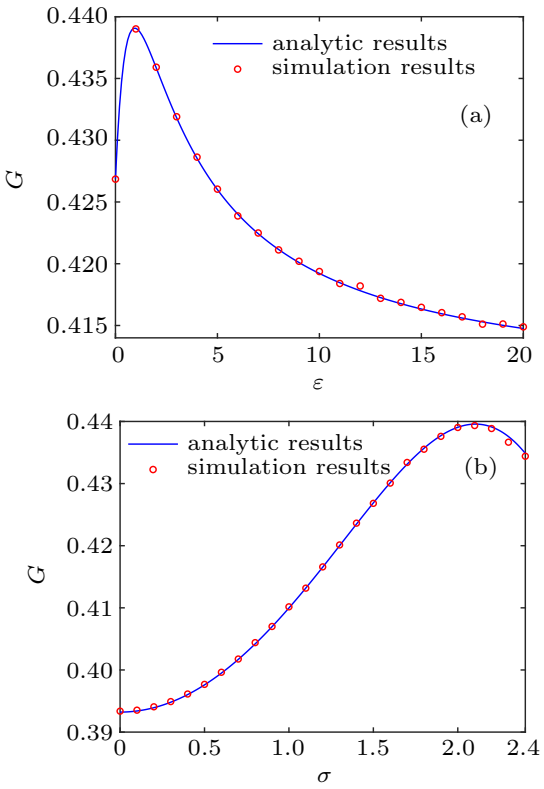


Fig. 8. Comparison of theoretical and simulation results, with (a) $\sigma = 2$ and the other system parameters being the same as Fig. 7(a); (b) $\varepsilon = 1$ and the other system parameters being the same as Fig. 7(b).

6. Discussion and conclusion

In this paper, the two coupled harmonic oscillators with dichotomous fluctuating frequency were investigated. First, the synchronization between the two particles and the synchronization condition were derived. Then the stability condition and the OAG of the coupled system were obtained. Based on these theoretical results, we analyzed the collective behaviors of the system, including stability, synchronization, and SR.

The synchronization means that, the mean field behavior is consistent with the behavior of any single particle in this coupled system. Therefore, to study the mean-field behavior of the system, we can only study the behavior of the first particle. Moreover, synchronization allows us to obtain exact steady-state solutions of the system, which provides a theoretical basis for the follow-up research on the collective behaviors.

Comparative analysis shows that, the stability condition is stronger than the synchronization condition, that is to say, when the stability condition is satisfied, the system is simultaneously synchronous and stable. In this situation, the system output is bounded, and through simulation analysis, it is found that the coupling strength has an important effect on the synchronization behavior. The bigger the coupling strength is, the shorter the synchronization time is. This indicates that increasing the coupling strength will reduce the synchronization time.

In the weak coupling region, there is an optimal coupling strength that maximizes the OAG, thus the coupling-induced SR behavior occurs. In the strong coupling region, the two particles are bounded as a whole, so that the coupling's effect gradually disappears. Coupling will also affect the system's traditional SR behavior. As the coupling strength increases, the resonance intensity first increases and then decreases. This indicates that there is an optimal coupling strength that maximizes the traditional SR behavior.

The model of this paper is just a basis case with linear coupling form and minimum system size. The collective behaviors of more complex coupled systems remain problems that require further research. We will extend the results of this paper to more complex situations in our future research.

Appendix A: Derivation of the synchronization condition (13)

In this section,we derive the synchronization condition (13). Using Eq. (12), we rewrite the SES as follow:

$$\boldsymbol{C}\frac{\mathrm{d}\boldsymbol{Z}}{\mathrm{d}t}+\boldsymbol{B}\boldsymbol{Z}=0, \tag{A1}$$

where

$$\boldsymbol{C}=\begin{pmatrix}1&0&0&0\\0&1&1&0\\0&0&0&1\\0&1&0&0\end{pmatrix},\quad \boldsymbol{Z}=\begin{pmatrix}z_1\\z_2\\z_3\\z_4\end{pmatrix},$$
$$\boldsymbol{B}=\begin{pmatrix}\omega+2\varepsilon&1&0&0\\\sigma^2&\lambda+\omega+2\varepsilon&\lambda+\omega+2\varepsilon&1\\0&0&\sigma^2&2\lambda+\omega+2\varepsilon\\\sigma^2&\lambda+\omega+\varepsilon&\varepsilon&0\end{pmatrix}. \tag{A2}$$

From Eq. (A1), we get the characteristic equation of the SES as follows:

$$\det(s\boldsymbol{C}+\boldsymbol{B})=\begin{vmatrix}s+\omega+2\varepsilon&1&0&0\\\sigma^2&s+\lambda+\omega+2\varepsilon&s+\lambda+\omega+2\varepsilon&1\\0&0&\sigma^2&s+2\lambda+\omega+2\varepsilon\\\sigma^2&s+\lambda+\omega+\varepsilon&\varepsilon&0\end{vmatrix}=\sum_{i=0}^{4}b_i s^i, \tag{A3}$$

with

$$\begin{aligned}
b_0&=\sigma^4-(4\varepsilon^2+6\varepsilon\lambda+6\varepsilon\omega+2\lambda^2+4\lambda\omega+2\omega^2)\sigma^2\\
&\quad+8\varepsilon^3\lambda+8\varepsilon^3\omega+12\varepsilon^2\lambda^2+24\varepsilon^2\lambda\omega\\
&\quad+12\varepsilon^2\omega^2+4\varepsilon\lambda^3+16\varepsilon\lambda^2\omega+18\varepsilon\lambda\omega^2\\
&\quad+6\varepsilon\omega^3+2\lambda^3\omega+5\lambda^2\omega^2+4\lambda\omega^3+\omega^4,\\
b_1&=-(6\varepsilon+4\lambda+4\omega)\sigma^2+8\varepsilon^3+24\varepsilon^2\lambda+24\varepsilon^2\omega\\
&\quad+16\varepsilon\lambda^2+36\varepsilon\lambda\omega+18\varepsilon\omega^2\\
&\quad+2\lambda^3+10\lambda^2\omega+12\lambda\omega^2+4\omega^3,\\
b_2&=-2\sigma^2+12\varepsilon^2+18\varepsilon\lambda+18\varepsilon\omega+5\lambda^2+12\lambda\omega+6\omega^2,\\
b_3&=6\varepsilon+4\lambda+4\omega,\\
b_4&=1.
\end{aligned} \tag{A4}$$

Based on the Routh–Hurwitz stability criterion, we can obtain the stability conditions of the SES in the following inequations:

$$\begin{cases}b_1b_4<b_2b_3,\\b_0b_3^2<b_1b_2b_3-b_1^2b_4,\\b_0>0,\\b_1>0,\\b_2>0.\end{cases} \tag{A5}$$

Then, by simplifying Eq. (A5), the stability conditions of the SES as the function of σ can be written as follows:

$$\begin{cases}\sigma<\sigma_{\mathrm{sy1}},\\\sigma<\sigma_{\mathrm{sy2}},\\\sigma<\sigma_{\mathrm{sy3}}\quad\text{or}\quad\sigma>\sigma_{\mathrm{sy4}},\\\sigma<\sigma_{\mathrm{sy5}},\\\sigma<\sigma_{\mathrm{sy6}},\end{cases} \tag{A6}$$

where

$$\sigma_{\mathrm{sy1}}=\sqrt{\frac{(\lambda+\omega+2\varepsilon)(16\varepsilon^2+25\varepsilon\lambda+25\varepsilon\omega+9\lambda^2+20\lambda\omega+10\omega^2)}{3\varepsilon+2\lambda+2\omega}},\quad \sigma_{\mathrm{sy2}}=\sqrt{\frac{a}{b}},$$

$$\sigma_{\mathrm{sy3}}=\sqrt{(\lambda+2\varepsilon+\omega)(\lambda+\varepsilon+\omega)-\sqrt{(\lambda+2\varepsilon+\omega)(2\varepsilon^3+(\lambda+\omega)\varepsilon^2+\lambda^2(\lambda+\omega))}},$$

$$\sigma_{\mathrm{sy4}}=\sqrt{(\lambda+2\varepsilon+\omega)(\lambda+\varepsilon+\omega)+\sqrt{(\lambda+2\varepsilon+\omega)(2\varepsilon^3+(\lambda+\omega)\varepsilon^2+\lambda^2(\lambda+\omega))}},$$

$$\sigma_{\mathrm{sy5}}=\sqrt{\frac{4\varepsilon^3+(12\lambda+12\omega)\varepsilon^2+(8\lambda^2+18\lambda\omega+9\omega^2)\varepsilon+\lambda^3+5\lambda^2\omega+6\lambda\omega^2+2\omega^3}{3\varepsilon+2\lambda+2\omega}},$$

$$\sigma_{\mathrm{sy6}}=\sqrt{6\varepsilon^2+9\varepsilon\lambda+9\varepsilon\omega+(5/2)\lambda^2+6\lambda\omega+3\omega^2},$$

$$\begin{aligned}a=&(2\varepsilon+2\omega+\lambda)(\varepsilon+\lambda+\omega)(\lambda+\omega+2\varepsilon)(2\varepsilon+2\omega+3\lambda)(4\varepsilon+2\omega+3\lambda)\\&(3\lambda^2+4(3\varepsilon+2\omega)\lambda+4(2\varepsilon+\omega)(\varepsilon+\omega))(4\varepsilon+2\omega+\lambda),\\ b=&(8\varepsilon^2+12\varepsilon\lambda+12\varepsilon\omega+3\lambda^2+8\lambda\omega+4\omega^2)(3\varepsilon+2\lambda+2\omega).\end{aligned}\tag{A8}$$

Since $\varepsilon,\sigma,\lambda,\omega$ are all positive numbers, through direct calculation, we have

$$\sigma^*=\min_{1\le i\le 6}\{\sigma_{\mathrm{sy}i}\}=\sigma_{\mathrm{sy3}}.\tag{A8}$$

In conclusion, the stability condition of the SES can be written as follows:

$$\sigma<\sigma^*=\sqrt{(\lambda+2\varepsilon+\omega)(\lambda+\varepsilon+\omega)-\sqrt{(\lambda+2\varepsilon+\omega)(2\varepsilon^3+(\lambda+\omega)\varepsilon^2+\lambda^2(\lambda+\omega))}},\tag{A9}$$

which is the synchronization condition (13).

Appendix B: The derivation of stability condition (23)

In this section, the stability condition (23) is derived. Using Eq. (22), we rewrite the OAGES as follows:

$$\frac{\mathrm{d}\boldsymbol{Y}}{\mathrm{d}t}+\boldsymbol{A}\boldsymbol{Y}=\boldsymbol{F},\tag{B1}$$

where

$$\boldsymbol{Y}=\begin{pmatrix}y_1\\y_2\\y_3\\y_4\end{pmatrix},\quad \boldsymbol{A}=\begin{pmatrix}\omega & 1 & 0 & 0\\ \sigma^2 & \lambda+\omega+\varepsilon & -\varepsilon & 0\\ 0 & -\varepsilon & \lambda+\omega+\varepsilon & 1\\ 0 & 0 & \sigma^2 & 2\lambda+\omega\end{pmatrix},\quad \boldsymbol{F}=\begin{pmatrix}A_0\cos(\Omega t)\\0\\0\\0\end{pmatrix}.\tag{B2}$$

Based on Eq. (B1), the characteristic equation is

$$\det(s\boldsymbol{I}+\boldsymbol{A})=\begin{vmatrix}s+\omega & 1 & 0 & 0\\ \sigma^2 & s+\lambda+\omega+\varepsilon & -\varepsilon & 0\\ 0 & -\varepsilon & s+\lambda+\omega+\varepsilon & 1\\ 0 & 0 & \sigma^2 & 2\lambda+s+\omega\end{vmatrix}=\sum_{i=0}^{4}a_i s^i,\tag{B3}$$

with

$$\begin{aligned}a_0&=4\varepsilon\lambda^2\omega+6\varepsilon\lambda\omega^2-2\varepsilon\lambda\sigma^2+2\varepsilon\omega^3-2\varepsilon\omega\sigma^2+2\lambda^3\omega+5\lambda^2\omega^2-2\lambda^2\sigma^2+4\lambda\omega^3-4\lambda\omega\sigma^2+\omega^4-2\omega^2\sigma^2+\sigma^4,\\ a_1&=4\varepsilon\lambda^2+12\varepsilon\lambda\omega+6\varepsilon\omega^2-2\varepsilon\sigma^2+2\lambda^3+10\lambda^2\omega+12\lambda\omega^2-4\lambda\sigma^2+4\omega^3-4\omega\sigma^2,\\ a_2&=6\varepsilon\lambda+6\varepsilon\omega+5\lambda^2+12\lambda\omega+6\omega^2-2\sigma^2,\\ a_3&=2\varepsilon+4\lambda+4\omega,\quad a_4=1.\end{aligned}\tag{B4}$$

Using the Routh–Hurwitz stability criterion, the stability condition for the OAGES is as follows:

$$\begin{cases} a_1a_4 < a_2a_3, \\ a_0a_3^2 < a_1a_2a_3 - a_1^2a_4, \\ a_0 > 0, \\ a_1 > 0, \\ a_2 > 0. \end{cases} \tag{B5}$$

By using Eq. (B4) to simplify Eq. (B5), the stability conditions for the OAGES as the function of σ can be written as follows:

$$\begin{cases} \sigma < \sigma_1, \\ \sigma < \sigma_2, \\ \sigma < \sigma_3 \quad \text{or} \quad \sigma > \sigma_4, \\ \sigma < \sigma_5, \\ \sigma < \sigma_6. \end{cases} \tag{B6}$$

where

$$\begin{aligned} \sigma_1 &= \sqrt{\frac{(\lambda+\omega)(6\varepsilon^2+15\varepsilon\lambda+15\varepsilon\omega+9\lambda^2+20\lambda\omega+10\omega^2)}{\varepsilon+2\lambda+2\omega}}, \\ \sigma_2 &= \sqrt{\frac{(2\omega+3\lambda)(2\omega+\lambda)(\lambda+\omega)(\omega+\varepsilon+\lambda)(2\omega+2\varepsilon+\lambda)(2\omega+2\varepsilon+3\lambda)}{(4\varepsilon\lambda+4\varepsilon\omega+3\lambda^2+8\lambda\omega+4\omega^2)(\varepsilon+2\lambda+2\omega)^2}}, \\ \sigma_3 &= \sqrt{(\lambda+\omega)(\lambda+\omega+\varepsilon) - \sqrt{(\lambda^3+(\omega+2\varepsilon)\lambda^2+\varepsilon^2\lambda+\varepsilon^2\omega)(\lambda+\omega)}}, \\ \sigma_4 &= \sqrt{(\lambda+\omega)(\lambda+\omega+\varepsilon) + \sqrt{(\lambda^3+(\omega+2\varepsilon)\lambda^2+\varepsilon^2\lambda+\varepsilon^2\omega)(\lambda+\omega)}}, \\ \sigma_5 &= \sqrt{\frac{\lambda^3+(5\omega+2\varepsilon)\lambda^2+6\omega(\omega+\varepsilon)\lambda+2\omega^3+3\varepsilon\omega^2}{\varepsilon+2\lambda+2\omega}}, \quad \sigma_6 = \sqrt{\frac{5}{2}\lambda^2+(6\omega+3\varepsilon)\lambda+3\omega(\omega+\varepsilon)}. \end{aligned} \tag{B7}$$

Since ε, σ, λ, ω are all positive numbers, through direct calculation, we have

$$\sigma_3 < \sigma_2 < \sigma_1, \quad \sigma_3 < \sigma_5 < \sigma_4 < \sigma_6. \tag{B8}$$

Let

$$\sigma^{**} = \min_{1\le i\le 6}\{\sigma_i\} = \sigma_3. \tag{B9}$$

In conclusion, the stability conditions of OAGES can be written as follows:

$$\sigma < \sigma^{**} = \sqrt{(\lambda+\omega)(\lambda+\omega+\varepsilon) - \sqrt{(\lambda^3+(\omega+2\varepsilon)\lambda^2+\varepsilon^2\lambda+\varepsilon^2\omega)(\lambda+\omega)}}. \tag{B10}$$

Appendix C: Comparison of stability condition and synchronization condition

In this section, we will derive the following conclusion: the stability condition (23) is stronger than the synchronization condition (13).

Proof We only need to prove $\sigma^{**} < \sigma^*$ (Eqs. (A9) and (B10)). We abbreviate σ^*, σ^{**} (Eqs. (A8) and (B9)) as

$$\begin{aligned} \sigma^{**} &= \sigma_3 = \sqrt{\sigma_{3,1} - \sqrt{\sigma_{3,2}}}, \\ \sigma^{*} &= \sigma_{\text{sy3}} = \sqrt{\sigma_{\text{sy3},1} - \sqrt{\sigma_{\text{sy3},2}}}, \end{aligned} \tag{C1}$$

where

$$\begin{aligned} \sigma_{3,1} &= (\lambda+\omega)(\lambda+\omega+\varepsilon), \\ \sigma_{3,2} &= (\lambda^3+(\omega+2\varepsilon)\lambda^2+\varepsilon^2\lambda+\varepsilon^2\omega)(\lambda+\omega), \\ \sigma_{\text{sy3},1} &= (\lambda+2\varepsilon+\omega)(\lambda+\varepsilon+\omega), \\ \sigma_{\text{sy3},2} &= (\lambda+2\varepsilon+\omega)(2\varepsilon^3+(\lambda+\omega)\varepsilon^2+\lambda^2(\lambda+\omega)). \end{aligned} \tag{C2}$$

So we just need to prove

$$\sigma_{3,1} - \sqrt{\sigma_{3,2}} > \sigma_{\text{sy3},1} - \sqrt{\sigma_{\text{sy3},2}}, \tag{C3}$$

this is equivalent to prove

$$\sigma_{3,1} - \sigma_{\text{sy3},1} > \sqrt{\sigma_{3,2}} - \sqrt{\sigma_{\text{sy3},2}}. \tag{C4}$$

Since

$$\begin{aligned} \sigma_{3,1} - \sigma_{\text{sy3},1} &= 2\varepsilon^2+2\varepsilon\lambda+2\varepsilon\omega > 0, \\ \sigma_{3,2} - \sigma_{\text{sy3},2} &= 4\varepsilon^4+4\varepsilon^3\lambda+4\varepsilon^3\omega > 0. \end{aligned} \tag{C5}$$

This is equivalent to prove

$$\begin{aligned} &(\sigma_{3,1} - \sigma_{\text{sy3},1})^2 > (\sqrt{\sigma_{3,2}} - \sqrt{\sigma_{\text{sy3},2}})^2 \\ &= \sigma_{3,2} + \sigma_{\text{sy3},2} - 2\sqrt{\sigma_{3,2}\sigma_{\text{sy3},2}}. \end{aligned} \tag{C6}$$

This is equivalent to prove

$$2\sqrt{\sigma_{3,2}\sigma_{\text{sy3},2}} > \sigma_{3,2} + \sigma_{\text{sy3},2} - (\sigma_{3,1} - \sigma_{\text{sy3},1})^2. \tag{C7}$$

By direct calculation, we have

$$4\sigma_{3,2}\sigma_{\mathrm{sy}3,2}-(\sigma_{3,2}+\sigma_{\mathrm{sy}3,2}-(\sigma_{3,1}-\sigma_{\mathrm{sy}3,1})^2)^2$$
$$=16\varepsilon^2\lambda^2(\omega+\lambda)(\omega+\lambda+2\varepsilon)(\omega+\lambda+\varepsilon)^2>0. \quad \text{(C8)}$$

Thus, the conclusion is proved.

References

[1] Benzi R, Sutera A and Vulpiani A 1981 *J. Phys. A* **14** L453
[2] Benzi R, Parisi G, Sutera A and Vulpiani A 1982 *Tellus* **34** 10
[3] Nicolis C 1982 *Tellus* **34** 1
[4] Gammaitoni L, Haänggi P, Jung P and Marchesoni F 1998 *Rev. Mod. Phys.* **70** 223
[5] Haänggi P, Jung P, Zerbe C and Moss F 1993 *J. Stat. Phys.* **70** 25
[6] McNamara B and Wiesenfeld K 1989 *Phys. Rev. A* **39** 4854
[7] Fox R F 1989 *Phys. Rev. A* **39** 4148
[8] Gang H, Ditzinger T, Ning C Z and Haken H 1993 *Phys. Rev. Lett.* **71** 807
[9] Tessone C J, Mirasso C R, Toral R and Gunton J D 2006 *Phys. Rev. Lett.* **97** 194101
[10] Atsumi Y, Hata H and Nakao H 2013 *Phys. Rev. E* **88** 052806
[11] Tang Y, Zou W, Lu J and Kurths J 2012 *Phys. Rev. E* **85** 046207
[12] Pikovsky A, Zaikin A and de la Casa M A 2002 *Phys. Rev. Lett.* **88** 050601
[13] Cubero D 2008 *Phys. Rev. E* **77** 021112
[14] Li J H 2002 *Phys. Rev. E* **66** 031104
[15] Gitterman M 2005 *Physica A* **352** 309
[16] Li J H and Han Y X 2006 *Phys. Rev. E* **74** 051115
[17] Li J H and Han Y X 2007 *Commun. Theor. Phys.* **47** 672
[18] Jiang S, Guo F, Zhou Y and Gu T 2007 *Physica A* **375** 483
[19] Li J H 2011 *Chaos* **21** 043115
[20] He G T, Tian Y and Wang Y 2013 *J. Stat. Mech.* **9** 26
[21] He G T, Luo R Z and Luo M K 2013 *Phys. Scr.* **88** 065009
[22] Yu T, Zhang L and Luo M K 2013 *Phys. Scr.* **88** 045008
[23] He G T, Tian Y and Luo M K 2014 *J. Stat. Mech.* **2014** P05018
[24] Zhong S C, Ma H, Peng H and Zhang L 2015 *Nonlinear Dyn.* **82** 535
[25] Chandrasekhar S 1943 *Rev. Mod. Phys.* **15** 1
[26] Sauga A, Mankin R and Ainsaar A 2012 *AIP Conf. Proc.* **1487** 224
[27] Lang R L, Yang L, Qin H L and Di G H 2012 *Nonlinear Dyn.* **69** 1423
[28] Mankin R, Laas K, Laas T and Reiter E 2008 *Phys. Rev. E* **78** 031120
[29] Soika R, Mankin R and Ainsaar A 2010 *Phys. Rev. E* **81** 011141
[30] Laas K, Mankin R and Rekker A 2009 *Phys. Rev. E* **79** 051128
[31] Yang B, Zhang X, Zhang L and Luo M K 2016 *Phys. Rev. E* **94** 022119
[32] Boccaletti S, Latora V, Moreno Y, Chavez M and Hwang D U 2006 *Phys. Rep.* **424** 175
[33] Nicolis C and Nicolis G 2017 *Phys. Rev. E* **96** 042214
[34] Droste F and Lindner B 2014 *Biol. Cybern.* **108** 825
[35] Reimann P and Elston T C 1996 *Phys. Rev. Lett.* **77** 5328
[36] Si M, Conrad N, Shin S, Gu J, Zhang J, Alam M and Ye P 2015 *IEEE Trans. Electron Dev.* **62** 3508
[37] Van Den Broeck C 1983 *J. Stat. Phys.* **31** 467
[38] Vishwamittar, Batra P and Chopra R 2021 *Physica A* **561** 125148
[39] Wojciech S and Dariusz W 2020 *Commun. Nonlinear Sci. Numer. Simulat.* **83** 105099
[40] Emelyanov Y P, Emelyanov V V and Ryskin N M 2014 *Commun. Nonlinear Sci. Numer. Simulat.* **19** 3778
[41] Shapiro V E and Loginov V M 1978 *Physica A* **91** 563
[42] Dorf R C and Bishop R H 2010 *Modern Control Systems*, 12th edn. (Pearson: Prentice Hall)
[43] Fulinski A 1993 *Phys. Lett. A* **180** 94
[44] Robertson B and Astumian R D 1991 *J. Chem. Phys.* **94** 7414
[45] Kubo R 1963 *J. Math. Phys* **4** 174
[46] Berdichevsky V and Gitterman M 1996 *Europhys. Lett* **36** 161
[47] Jiang S Q, Hou M J, Jia C H, He J R and Gu T X 2009 *Chin. Phys. B* **18** 2667
[48] Astumian R D and Bier M 1994 *Phys. Rev. Lett.* **72** 1766
[49] Li J H and Huang Z Q 1998 *Phys. Rev. E* **57** 3917
[50] Bier M 1997 *Contemp. Phys.* **38** 371
[51] Li J H, Chen Q H and Zhou X F 2010 *Phys. Rev. E* **81** 041104
[52] Wang Q, Perc M, Duan Z and Chen G 2009 *Chaos* **19** 023112
[53] Hendricks A G, Epureanu B I and Meyhofer E 2009 *Phys. Rev. E* **79** 031929
[54] Stukalin E B, Phillips III H and Kolomeisky A B 2005 *Phys. Rev. Lett.* **94** 238101
[55] Kim C, Lee E K and Talkner P 2006 *Phys. Rev. E* **73** 026101